Molecular Therapy
Original Article

FOXO3A-induced LINC00926 suppresses breast tumor growth and metastasis through inhibition of PGK1-mediated Warburg effect

Zhong Chu,[1,5] Nan Huo,[2,5] Xiang Zhu,[2,5] Hanxiao Liu,[1] Rui Cong,[2] Luyuan Ma,[2] Xiaofeng Kang,[2] Chunyuan Xue,[2] Jingtong Li,[2] Qihong Li,[3] Hua You,[4] Qingyuan Zhang,[1] and Xiaojie Xu[2]

[1]Department of Medical Oncology, Harbin Medical University Cancer Hospital, Harbin, Heilongjiang 150081, China; [2]Department of Cellular Engineering Lab, Beijing Institute of Biotechnology, Beijing 100850, China; [3]Department of Stomatology, Fifth Medical Center of Chinese PLA General Hospital, Beijing 100071, China; [4]Department of Oncology, Affiliated Cancer Hospital & Institute of Guangzhou Medical University, Guangzhou 510095, China

Phosphoglycerate kinase 1 (PGK1), a critical component of the glycolytic pathway, relates to the development of various cancers. However, the mechanisms of PGK1 inhibition and physiological significance of PGK1 inhibitors in cancer cells are unclear. Long non-coding RNAs (lncRNAs) play a vital role in tumor growth and progression. Here, we identify a lncRNA LINC00926 that negatively regulates PGK1 expression and predicts good clinical outcome of breast cancer. LINC00926 downregulates PGK1 expression through the enhancement of PGK1 ubiquitination mediated by E3 ligase STUB1. Moreover, hypoxia inhibits LINC00926 expression and activates PGK1 expression largely through FOXO3A. FOXO3A/LINC00926/PGK1 axis regulates breast cancer glycolysis, tumor growth, and lung metastasis both in *vitro* and in *vivo*. In breast cancer patients, LINC00926 expression is negatively correlated with PGK1 and positively correlated with FOXO3A expression. Our work established FOXO3A/LINC00926/PGK1 as a critical axis to regulate breast cancer growth and progression. Targeting PGK1 or supplement of LINC00926 or FOXO3A could be potential therapeutic strategies in breast cancer.

INTRODUCTION

Although great progress has been made in breast cancer research and therapy in recent years, the morbidity and mortality of breast cancer are still rising, making it a major threat to women's health. Energy metabolism reprogramming is featured by a state termed "Warburg effect," widely acknowledged as an emerging hallmark in cancers, exhibits aberrant metabolism characterized by high glycolysis regardless of the presence of abundant oxygen.[1] This glycolytic process is usually accompanied by glucose uptake and lactate production, as well as ATP generation, facilitating tumor growth and progression. Thus, glycolytic enzymes, which affect the critical stage of the process, play key roles in cancer cell growth and progression and become potential targets for cancer treatment.[2]

Phosphoglycerate kinase 1 (PGK1), a critical component of the glycolytic pathway, is a rate-limiting enzyme that catalyzes the conversion of 1, 3-bisphospholgycerate (1, 3-BPG) and ADP into 3-phosphoglycerate (3-PG) and ATP. This PGK1-catalyzed reaction is the first ATP-yielding step of glycolysis and is essential for energy production in most living cells. PGK1 mediates glycolysis that generates ATP for tumor cells especially under hypoxic conditions, which is related to the development of various cancers.[3] High PGK1 predicts poor survival in breast cancer, head and neck cancer, cervical cancer, liver cancer, and pancreatic cancer.[4–6] Therefore, PGK1 has gradually become a focused target in cancer research. Expression of PGK1 is stimulated by several known oncogenes or transcription factors, such as MYC and hypoxia inducible factor 1 α (HIF-1α).[7,8] However, the mechanisms of PGK1 inhibition and the physiological significance of the PGK1 inhibitors in cancer cells are unclear.

Long non-coding RNAs (lncRNAs) are a recently discovered major class of non-coding RNAs with a length of more than 200 nt.[9] Mechanistically, lncRNAs exert their function by regulating gene expression in different levels, including epigenetic modulation, transcriptional (or post transcriptional), and translational regulation. It has been demonstrated that lncRNAs are involved in a variety of cellular biological functions, such as chromatin imprinting, cell differentiation, and tumor glycolysis, etc.[10] As for the regulation of PGK1 by lncRNA in tumorigenesis, Yu et al.[11] reported that MetaLnc9 interacts with PGK1 and upregulates PGK1 expression in non-small

Received 14 January 2021; accepted 27 April 2021;
https://doi.org/10.1016/j.ymthe.2021.04.036.

[5]These authors contributed equally

Correspondence: Qingyuan Zhang, Department of Medical Oncology, Harbin Medical University Cancer Hospital, Harbin, Heilongjiang 150081, China.
E-mail: 0566@hrbmu.edu.cn
Correspondence: Xiaojie Xu, Department of Cellular Engineering Lab, Beijing Institute of Biotechnology, Beijing 100850, China.
E-mail: miraclexxj@126.com
Correspondence: Hua You, Department of Oncology, Affiliated Cancer Hospital & Institute of Guangzhou Medical University, Guangzhou 510095, China.
E-mail: youhua307@163.com
Correspondence: Qihong Li, Department of Stomatology, Fifth Medical Center of Chinese PLA General Hospital, Beijing 100071, China.
E-mail: liqihong@126.com

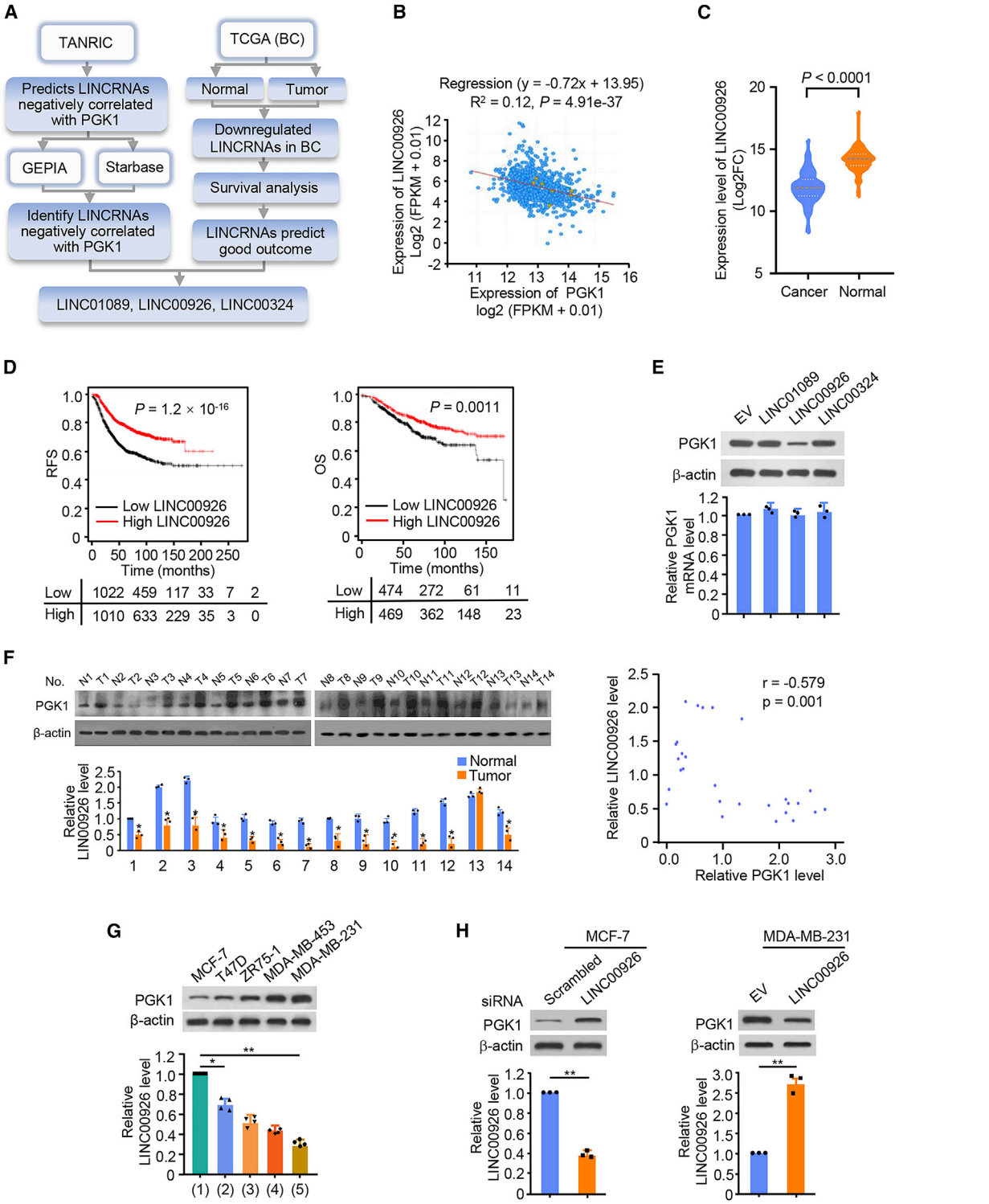

Figure 1. Identification of LINC00926 as a lncRNA downregulated in breast cancer and negatively correlated with PGK1

(A) Schematic diagram of screening strategy to identify lncRNAs downregulated in breast cancer (BC) and negatively correlated with PGK1. (B) Pearson's correlation analysis of LINC00926 and PGK1 expression in breast cancer tissues (https://www.cbioportal.org/). (C) LINC00926 expression in breast cancer patients and normal controls revealed by the TCGA database. (D) Kaplan-Meier plotter analysis of the correlation of LINC00926 expression level with relapse free survival (p = 1.2 × 10–16) or overall survival

(legend continued on next page)

cell lung cancer (NSCLC) cells, leading to promotions of NSCLC cell migration and invasion. Cai et al.[12] reported that GBCDRlnc1 interacts with PGK1 and activates autophagy at the initial stage, thus reducing the sensitivity of Dox-resistant gallbladder cancer cells. lncRNA MSC-AS1 promoted hepatocellular carcinoma (HCC) oncogenesis via inducing the expression of PGK1[13] and LINC01559 accelerated gastric cancer progression via upregulation of PGK1.[14] Collectively, currently reported lncRNAs that target PGK1 are positive regulators, however, negatively regulated lncRNAs still remain unknown. Therefore, exploring lncRNAs that negatively regulate PGK1 expression is of great importance and have more clinical therapeutic value. In addition, the detailed mechanistical and functional study, the clinical significance, and the upstream lncRNAs that regulate PGK1 in breast cancer remain unknown.

Homo sapiens long intergenic non-protein coding RNA 00926 (LINC00926) is a lncRNA that produces a 2.53 kb transcript, the biological role of which is unknown. In the current study, we identify a lncRNA LINC00926 that negatively regulates PGK1 expression and predicts good clinical outcome of breast cancer. Mechanistically, LINC00926 downregulates PGK1 expression by enhancing the ubiquitination of PGK1 mediated by the E3 ligase STUB1. Moreover, hypoxia inhibits LINC00926 expression and activates PGK1 expression largely through transcription factor FOXO3A. FOXO3A/LINC 00926/PGK1 axis regulates breast cancer glycolysis, tumor growth, and lung metastasis both in *vitro* and in *vivo*. Our work established FOXO3A/LINC00926/PGK1 as a critical axis to regulate breast cancer growth and progression.

RESULTS

LINC00926 is screened out as PGK1 negatively regulated lncRNA and associated with breast cancer clinical outcome

The coding potential of LINC00926 transcript was determined using the Coding Potential Assessment Tool (CPAT), the Coding Potential Calculator (CPC), and PhyloCSF codon substitution frequency analysis. These data strongly suggested that LINC00926 is a non-coding RNA (Figures S1A–S1C). To explore lncRNAs negatively regulating PGK1, we analyzed the three databases of breast cancer according to the screening strategy shown in Figure 1A. Briefly, we screened the negatively correlated-PGK1 lncRNAs in TANRIC database, compared the expression of lncRNAs in normal and cancer tissues, and analyzed the survival of lncRNAs in Starbase and TCGA database. We identified three lncRNAs, LINC00926, LINC01089, and LINC00324 negatively correlated with PGK1 and exhibiting good clinical outcome (Figures 1B–1D; Figures S1A–S1H). To investigate whether the identified lncRNAs actually downregulate PGK1 expression, we transfected breast cancer cells with each of the three lncRNAs, respectively. Our result demonstrated that only LINC00926 led to a significant decrease in PGK1 protein level in both MCF-7 and MDA-MB-231 cells with the mRNA levels unchanged (Figure 1E; Figure S2I), suggesting that LINC00926 downregulates PGK1 expression in breast cancer cells.

To confirm the role of LINC00926 in breast cancer, we assessed the expression levels of PGK1 and LINC00926 in 14 pairs of breast cancer and their corresponding nontumorous tissues by western blot and real-time RT-PCR. Compared with their corresponding nontumorous counterparts, 13/14 (92.9%) of breast cancer cases had reduced LINC00926 expression while 12/14 (85.7%) had upregulated PGK1 expression. In agreement with LINC00926 inhibition of PGK1 in cultured cells, expression of LINC00926 was negatively correlated with PGK1 expression in breast cancer samples ($p = 0.001$, $r = -0.579$; Figure 1F). Interestingly, we found that endogenous PGK1 protein level and LINC00926 level were negatively expressed in five breast cancer cell lines (MCF-7, T47D, ZR75-1, MDA-MB-453, MDA-MB-231). The relatively metastatic cell line MDA-MB-231, which expressed PGK1 at the highest level, expressed LINC00926 at the lowest level while the less malignant cell line MCF-7, which expressed PGK1 at a relatively low level, expressed LINC00926 at a relatively high level (Figure 1G). Our result demonstrated that knockdown of LINC00926 with the specific smart silencers led to a marked increase in PGK1 expression in MCF-7 cells while overexpression of LINC00926 decreased that of PGK1 expression in MDA-MB-231 cells (Figure 1H). These results suggest that LINC00926 downregulates PGK1 expression and may be negatively involved in PGK1-mediated breast cancer development.

LINC00926 suppresses proliferation, migration, and invasion through inhibition of PGK1 expression in breast cancer cells

To investigate the biological functions of LINC00926 in breast cancer cells, we infected cells with LINC00926 and then subjected them to cell growth, migration, and invasion analysis. Cell proliferation and colony formation assays revealed that overexpression of LINC00926 reduced the proliferation of MDA-MB-231 and MCF-7 cells (Figures 2A and 2B; Figures S3A and S3B). These effects could be reversed by PGK1 reexpression in the LINC00926-transfected cell lines. LINC00926 overexpression also displayed decreased migration and invasion ability (Figures 2C and 2D; Figures S3C and S3D). Again, PGK1 reexpression in the LINC00926-transfected cells reversed these effects. Moreover, PGK1 knockdown abolished the ability of LINC00926 to regulate breast cancer cell proliferation, migration, and invasion (Figures 2E–2H; Figure S3E–S3H), indicating that

($p = 0.0011$) of breast cancer patients by the KM plotter (log-rank test, two-sided; http://kmplot.com/analysis/). (E) The protein levels and mRNA levels of PGK1 in MCF-7 cells transfected with empty vector, LINC01089, LINC000926, and LINC00324 expression vector. (F) Upper panels show the representative immunohistochemical (IHC) staining of PGK1 in cancerous breast tissues and adjacent normal breast tissues. LINC000926 expression in human cancerous breast tissues and adjacent normal breast tissues was plotted using real-time RT-PCR. Correlation of relative LINC00926 and PGK1 level is on the right side. (G) Expression of LINC00926 and PGK1 in different breast cancer cell lines were performed by quantitative real-time PCR or western blot. (H) Left panel shows the expression levels of PGK1 and LINC00926 in MCF-7 cells transfected with scrambled or LINC00926 siRNA. Right panel shows expression levels of PGK1 and LINC00926 in MDA-MB-231 cells transfected with empty vector and LINC00926 expression vector. The data are presented as the mean ± SD.

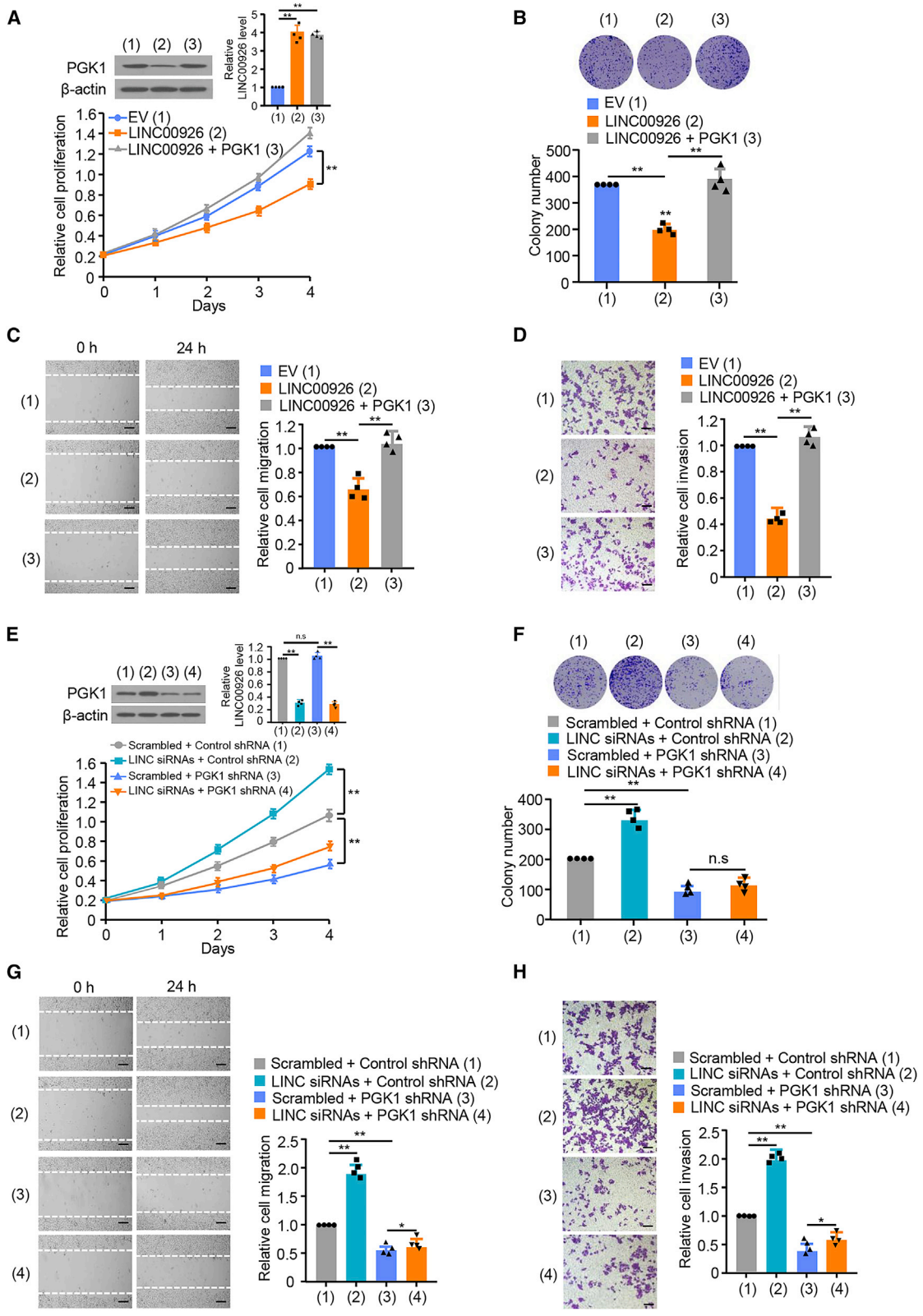

(legend on next page)

LINC00926 suppresses breast cancer cell proliferation, migration, and invasion through inhibition of PGK1 expression.

LINC00926 dampens glycolysis via inhibition of PGK1 expression in breast cancer cells

Since PGK1 is a critical glycolytic enzyme and LINC00926 is identified as a negatively PGK1-regulated lncRNA, we wondered whether aerobic glycolysis plays a role in LINC00926-mediated inhibition of breast cancer cell proliferation. Indeed, the glycolytic inhibitor 2-deoxy-D-glucose (2-DG) dampened the ability of LINC00926 to inhibit proliferation in MCF-7 and MDA-MB-231 cells, indicating that LINC00926 may participate in glycolysis of breast cancer cells (Figures S4A and S4B). Therefore, we tested the effect of LINC00926 on regulation of glucose uptake, lactate production, and ATP generation. As expected, LINC00926 decreased glucose uptake, lactate production, and ATP generation (Figure 3A; Figure S5A). These effects were reversed by PGK1 reexpression in the LINC00926-transfected cells. LINC00926 also displayed decreased extracellular acidification rate (ECAR), which reflects overall glycolytic flux, and increased oxygen consumption rate (OCR), an indicator of mitochondrial respiration (Figures 3B and 3C; Figures S5B and S5C). Again, PGK1 reexpression in the LINC00926-transfected cells rescued these effects. LINC00926 knockdown in the PGK1 knockdown MDA-MB-231 or MCF-7 cells had no effects on the glycolytic phenotype (Figures 3D–3F; Figures S5D–S5F), indicating that LINC00926 represses the glycolytic phenotype via PGK1. Taken together, these data collectively suggest that LINC00926 dampens glycolysis via inhibition of PGK1 expression in breast cancer cells.

LINC00926 regulates PGK1 protein stability through enhancing the STUB1-mediated ubiquitin-proteasome pathway

Subcellular localization results showed that LINC00926 was localized predominantly in the cytoplasm, which was further verified by RNA fluorescence *in situ* hybridization (FISH) assays (Figures 4A and 4B). Combined with the fact that LINC00926 did not alter PGK1 mRNA level, we speculated that LINC00926 downregulated PGK1 expression at the posttranscriptional level. Indeed, addition of the proteasome inhibitor MG132 blocked LINC00926 overexpression-mediated PGK1 degradation, suggesting that the ubiquitin-proteasome pathway is involved in LINC00926 modulation of PGK1 protein stability (Figure 4C). LINC00926 overexpression increased PGK1 ubiquitination (Figure 4D). LINC00926 knockdown, which increased PGK1 protein levels, decreased PGK1 ubiquitination (Figure 4E).

To search for the E3 ubiquitin ligase STUB1 responsible for LINC00926 modulation of PGK1 protein stability, we next identified protein partners of LINC00926 in breast cancer cells through RNA pull-down assays. The result demonstrated specific differentially expressed bands that were subjected to mass spectrometry. There were several potential LINC00926-interacting proteins identified based on unique peptides with repeated appearances, including two E3 ligases, STUB1 and E6AP (Figure 4F). Immunoblotting further confirmed that only STUB1 interacted with LINC00926, whereas E6AP didn't (Figure 4G). Moreover, RNA immunoprecipitation (RIP) assays also demonstrated that LINC00926 was markedly enriched in PGK1 and STUB1 immunoprecipitates (Figure 4H). PGK1 (1–369 nt), the substrate binding region, and STUB1 (220–304 nt), the *U*-BOX region, as determined by measuring coprecipitated RNA by qPCR, interacted with LINC00926 (Figure S6A). On the other hand, coimmunoprecipitation (coIP) assays demonstrated that LINC00926 (401–800 nt) interacted with PGK1 and LINC00926 (2,001–2,534 nt) interacted with STUB1 (Figure S6B). These results indicated that PGK1 and E3 ubiquitin ligase STUB1 specifically interact with LINC00926 in breast cancer cells. Intriguingly, LINC00926 enhanced STUB1-mediated PGK1 ubiquitination (Figure 4I). STUB1 knockdown greatly attenuated the effects of LINC00926 on PGK1 ubiquitination (Figure 4J). These data suggest that STUB1 plays a critical role in the regulation of PGK1 ubiquitination by LINC00926. Consistent with the effects of LINC00926 on STUB1-mediated PGK1 ubiquitination, LINC00926 increased the interaction between STUB1 and PGK1 (Figure 4K). These effects seem to be specific for STUB1, because LINC00926 did not alter the association of PGK1 with E6AP, another E3 ubiquitin ligase screened out for PGK1 (Figure S6C). Consistent with the ubiquitination results, STUB1 knockdown greatly attenuated the effects of LINC00926 on PGK1 degradation (Figure 4L).

Hypoxia inhibits LINC00926 expression and activates PGK1 expression largely through FOXO3A transcription

Since hypoxia is a key phenomenon in cancers, we determined whether the LINC00926/PGK1 axis plays a role in regulation of glycolysis under hypoxia. Interestingly, hypoxia stimulated PGK1 expression at both mRNA and protein levels and decreased LINC00926 expression (Figure 5A). To determine how hypoxia represses LINC00926 expression in breast cancer cells, we investigated repression of the LINC00926 promoter after hypoxia. Analysis of various LINC00926 promoter deletion reporter constructs showed that the promoter region from −300 to −200 bp contained a hypoxia-repressive element (Figure 5B). Mutation of a putative FOXO3A-binding site in this region predicted by a bioinformatics method (http://tfbind.hgc.jp) resulted in loss of the repression.

Figure 2. LINC00926 suppresses proliferation, migration, and invasion through inhibition of PGK1 expression in breast cancer cells

(A) MCF-7 cells were transfected with LINC00926 or LINC00926 plus PGK1 expression vector. The proliferation of the cells was detected by CCK-8 assay. The representative immunoblot shows PGK1 expression. Histograms show LINC00926 expression determined by quantitative real-time PCR. (B) Colony-formation assay of MCF-7 cells transfected as in (A). Representative images show colonies in plates (upper panels). Histograms show colony number. (C and D) Wound healing (C) and invasion (D) assays of MCF-7 cells transfected as in (A). Right histograms show relative cell migration and invasion. (E and F) Lentivirus-mediated PGK1 knockdown (PGK1 shRNA) or control MCF-7 cells were transfected with Scramble or LINC00926 siRNA and analyzed as in (A) and (B). (G and H) Wound healing (G) and invasion (H) assays of lentivirus-mediated PGK1 knockdown (PGK1 shRNA) or control MCF-7 cells were transfected as in (E) and (F). Scale bar, 50 μm. All values shown are mean ± SD of triplicate measurements and have been repeated 4 times with similar results (*$p < 0.05$, **$p < 0.01$ versus corresponding control).

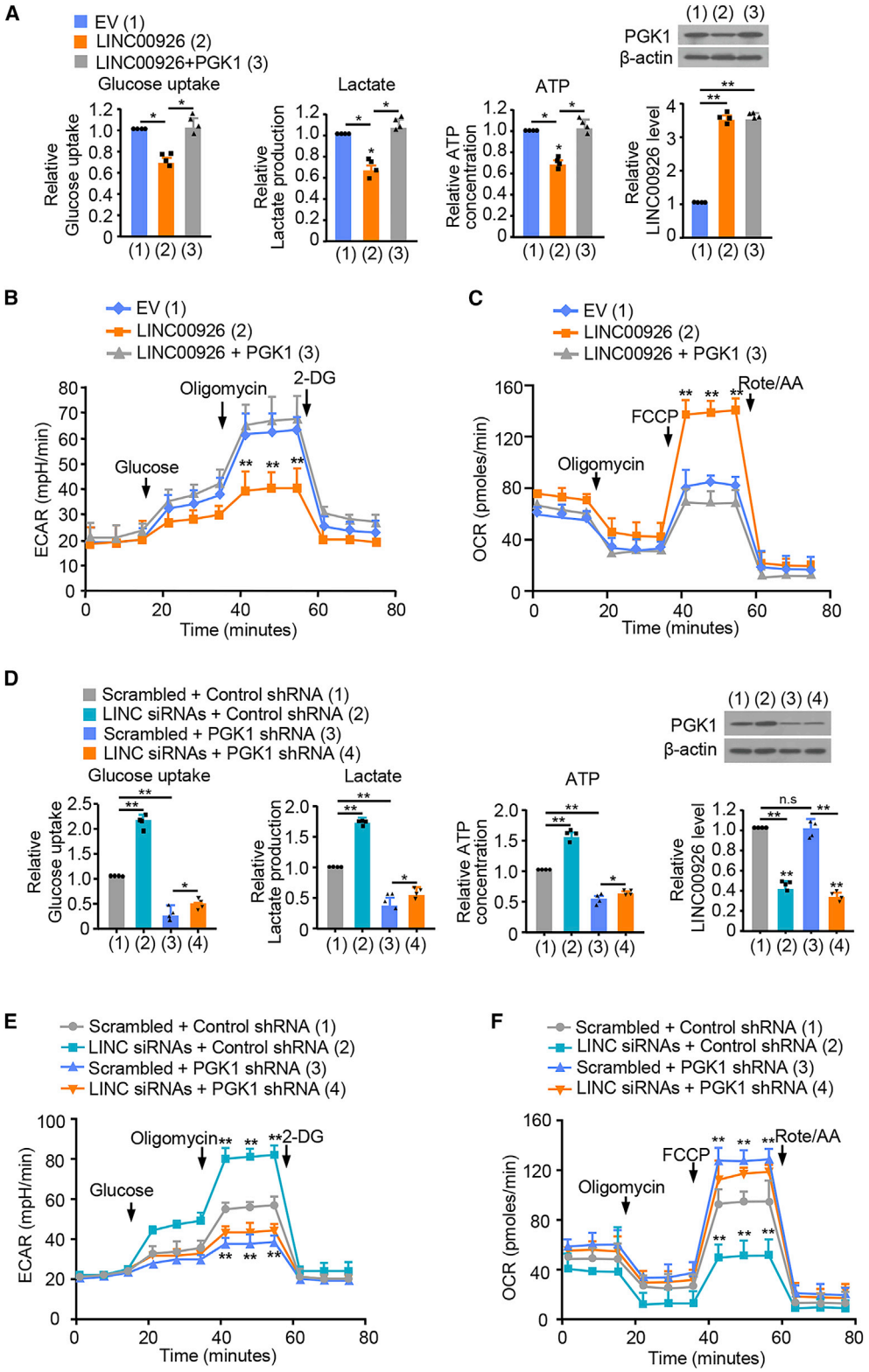

(legend on next page)

Indeed, under normoxia or hypoxia condition, FOXO3A instead of other FOXO family members affects LINC00926 and PGK1 expression, indicating that FOXO3A is the specific transcription factor for LINC00926 regulation (Figures 5C and 5D; Figure S7A). Chromatin immunoprecipitation (ChIP) assay demonstrated that, under normoxia, FOXO3A was recruited to the region containing the putative FOXO3A-binding site within the LINC00926 promoter, but not to a region upstream of the LINC00926 promoter, and the recruitment was decreased under hypoxia (Figure 5E). FOXO3A increased LINC00926 level and decreased PGK1 level, and importantly, LINC00926 knockdown greatly impaired the ability of FOXO3A to regulate LINC00926 and PGK1 expression under both normoxia or hypoxia condition (Figure 5F; Figure S7B). In addition, knockdown of LINC00926 greatly impaired the effect of hypoxia on PGK1 upregulation. These data suggest that hypoxia inhibits LINC00926 expression and activates PGK1 expression largely through FOXO3A transcription.

FOXO3A suppresses proliferation, migration, and invasion and dampens glycolysis via regulation of LINC00926 expression in breast cancer cells

We investigated whether FOXO3A regulates these effects through the LINC00926. Cell proliferation and colony-formation assays revealed that FOXO3A overexpression inhibited breast cancer cell growth while LINC00926 knockdown increased cell growth (Figures 6A and 6B; Figure S8A). Importantly, LINC00926 knockdown greatly attenuated the ability of FOXO3A to regulate cell proliferation, suggesting that FOXO3A decreased breast cancer cell proliferation largely through the LINC00926 expression.

Next, we determined whether FOXO3A inhibits cell migration, invasion, and glycolysis via LINC00926. As expected, FOXO3A reduced breast cancer cell migration and invasion (Figures 6C and 6D; Figures S8B and S8C). LINC00926 knockdown greatly attenuated the ability of FOXO3A to suppress cell migration and invasion. FOXO3A overexpression inhibited glucose uptake, lactate production, and ATP generation and displayed decreased ECAR and increased OCR. Importantly, LINC00926 knockdown greatly attenuated the ability of FOXO3A to regulate cell migration, invasion, and glycolysis (Figures 6C–6G; Figures S8D–S8F). Taken together, these results suggest that FOXO3A suppresses breast cancer cell migration and invasion, as well as glycolysis largely dependent on LINC00926.

FOXO3A/LINC00926/PGK1 axis regulates breast cancer tumor growth and lung metastasis

To confirm the *in vivo* phenotype of the FOXO3A/LINC00926/PGK1 pathway, we first investigated the effect of LINC00926/PGK1 axis on breast cancer growth by injecting MDA-MB-231 cells harboring the indicated constructs into the mammary fat pads of BALB/c mice. As expected, LINC00926 knockdown markedly increased breast tumor growth. On the contrary, tumor growth was suppressed when PGK1 was knocked down. More importantly, the effect of LINC00926 knockdown on tumor growth was dramatically attenuated when PGK1 was knocked down (Figures 7A–7C). Next, we investigated the FOXO3A/LINC00926 axis on breast cancer growth. The result showed that FOXO3A overexpression significantly decreased breast cancer growth. Tumor growth was increased when LINC00926 was knocked down. The effect of FOXO3A overexpression on tumor growth was dramatically attenuated when LINC00926 was knocked down (Figures 7D–7F).

Next, we examined the effect of the pathway on breast cancer metastasis. The number of the nodules spread throughout the pulmonary region was markedly increased in the LINC00926 knockdown group compared with that in control group (Figure 7G). In contrast, PGK1 knockdown led to a decrease in the metastatic spread of breast cancer cells to the lung. Importantly, PGK1 knockdown greatly attenuated the ability of LINC00926 knockdown to regulate lung metastasis (Figure 7G). Histologic analysis on the lungs confirmed the metastasis foci. Consistent with the results of the tumor growth experiments, LINC00926 knockdown markedly attenuated the ability of FOXO3A to regulate the lung metastasis (Figure 7H).

Correlation between LINC00926 and PGK1 expression and association of LINC00926 with glucose uptake in human breast cancer patients

We assessed PGK1 expression by immunohistochemical (IHC) staining and LINC00926 expression by FISH in 109 human breast cancer samples. In agreement with the LINC00926 inhibition of PGK1 in cultured cells, the expression of LINC00926 negatively correlated with PGK1 expression and positively related to FOXO3A (Figure 8A). Moreover, LINC00926 expression associated with tumor size, stage, ERα, PR, HER2, and event (Table S4). Importantly, patients with breast tumors who had increased glucose uptake assessed by ^{18}FDG PET scans showed decreased LINC00926 and FOXO3A expression and increased expression of PGK1 (Figure 8B). The specificity of LINC00926 was confirmed by FISH and the specificity of the PGK1 antibody was confirmed by IHC or immunoblot with cell lysates (Figure S9). Taken together, these data suggest important pathological roles of the LINC00926/PGK1 axis in breast cancer.

DISCUSSION

Cancer cells are characterized by an increase in glucose uptake and glycolysis.[1] Enzymes and products involved in this process have

Figure 3. LINC00926 dampens glycolysis via inhibition of PGK1 expression in breast cancer cells

(A) MCF-7 cells were transfected with LINC00926 or LINC00926 plus PGK1 expression vector. Glucose uptake and the production of lactate and ATP were determined. Representative immunoblot reveals the expression of PGK1. Quantitative real-time PCR analysis indicates LINC00926 expression. (B and C) MCF-7 cells were transfected as in (A), and extracellular acidification rate (ECAR) (B) and oxygen consumption rate (OCR) (C) were then determined. PGK1 shRNA or control MCF-7 cells were transfected with Scramble or LINC00926 siRNAs. (D) Glucose uptake and lactate production and ATP production were measured. Typical immunoblot reveals the expression of PGK1. Quantitative real-time PCR analysis shows LINC00926 expression. (E and F) ECAR (E) and OCR (F) assays of PGK1 shRNA or control MCF-7 cells were transfected as in (D). All values shown are mean ± SD of triplicate measurements and have been repeated 4 times with similar results (A–F). *$p < 0.05$, **$p < 0.01$ versus corresponding control.

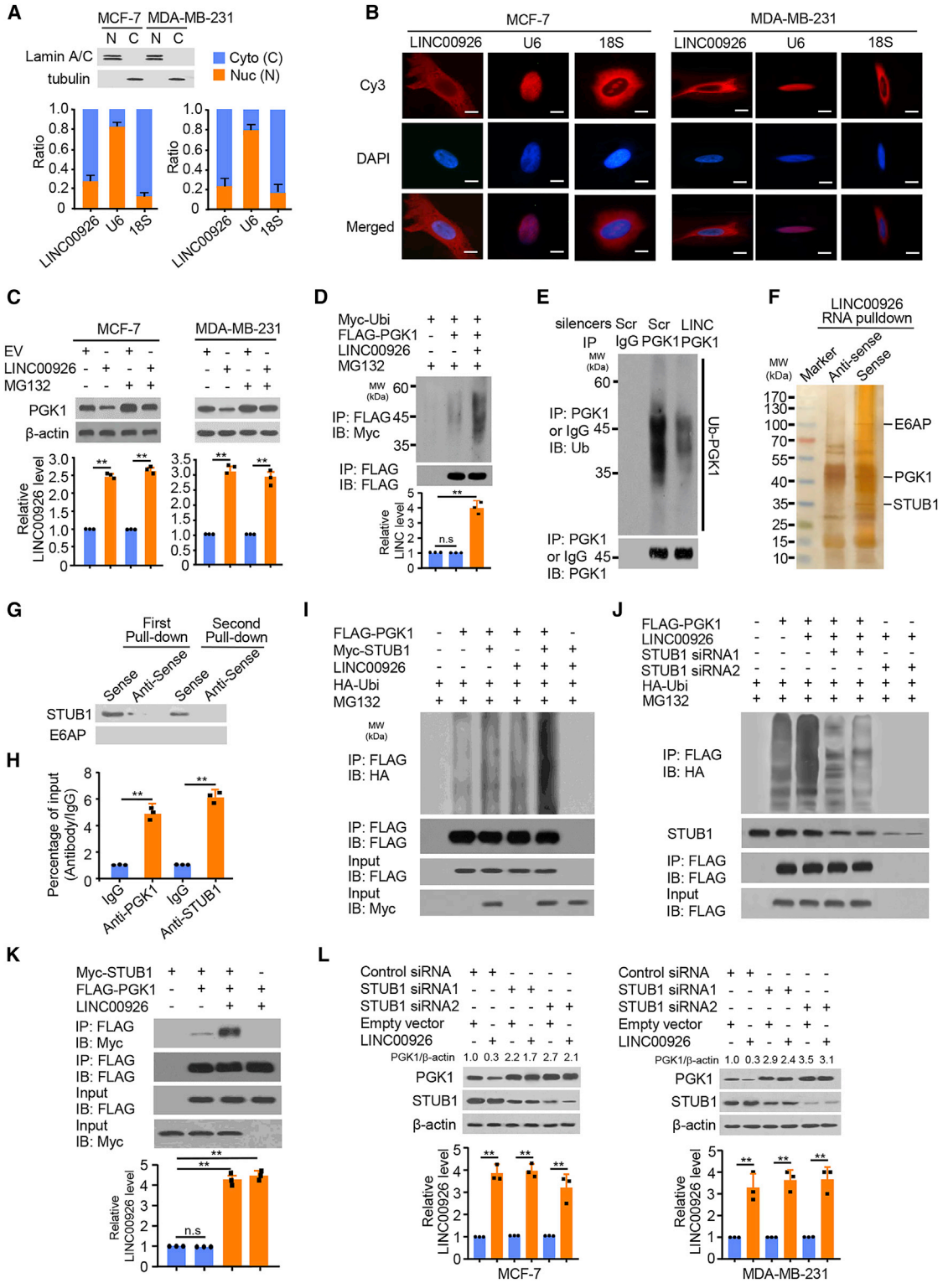

Figure 4. LINC00926 regulates PGK1 protein stability through enhancing the STUB1-mediated ubiquitin-proteasome pathway

(A) Expression of LINC00926 in MCF-7 and MDA-MB-231 cells was detected by quantitative real-time PCR. The separation of nucleus and cytoplasm was estimated by western blot. Lamin A/C was used as the nucleus marker and tubulin as the cytoplasm marker. (B) Subcellular localization of LINC00926 (red) in MCF-7 and MDA-MB-231

(legend continued on next page)

been proved to promote cancer aggressiveness.[15] Therefore, searching for new agents that target metabolic enzymes to block glucose metabolism or induce a switch from glycolysis to mitochondrial respiration is of great significance.

PGK1 plays a critical role in the glycolytic pathway, which is the first ATP-yielding step of glycolysis and is essential for energy production in cells. PGK1 is expressed in many solid cancer cells including breast cancer, and high PGK1 expression predicts poorer relapse-free and overall survival in breast cancer patients.[16,17] In addition, overexpression of PGK1 promotes cancer cell proliferation, invasion, and metastasis, which relates to the development and progress of breast cancers.[3,16] However, the upstream factors of PGK1 and how they control PGK1 expression remain largely unknown. Our study identified a FOXO3A/LINC00926/PGK1 axis to control breast cancer glycolysis, growth, and metastasis. FOXO3A and LINC00926 are upstream regulators of PGK1. In breast cancer cells, LINC00926 inhibits glucose uptake and lactate production, and induces a switch from glycolysis to mitochondrial respiration through inhibition of PGK1 expression. LINC00926 suppresses breast tumor growth and metastasis through inhibition of PGK1-mediated Warburg effect. We further showed that LINC00926 is a transcriptional target of FOXO3A. Moreover, in breast cancer samples, FOXO3A or LINC00926 expression is negatively correlated with PGK1 expression, as well as increased tumor FDG uptake. Thus, our data establish the physiological and pathological significance of FOXO3A or LINC00926 in regulating PGK1-mediated Warburg effect. LINC00926 or FOXO3A activation may be useful for treatment of breast cancer with PGK1 overexpression.

In recent years, lncRNAs have been identified as a new understanding of disease pathogenesis, involved in a variety of cellular biological functions, such as chromatin imprinting, cell differentiation and tumorigenesis, etc. lncRNAs are a major class of non-coding RNAs with a length of more than 200 nt. Mechanistically, lncRNAs exert their functions by regulating gene expression in different levels, including epigenetic modulation, transcription, post transcription, and translation regulation. Yu et al.[11] showed that LINC00963 post-translationally regulated PGK1 in NSCLC cells and enhanced the lung metastasis. Cai et al.[12] revealed that lncRNA GBCDRlnc1 directly interacts with PGK1 and regulates its stability, eventually leading to the increased the expression of ATG5-ATG12 conjugate. Wang et al.[14] reported that LINC01559 upregulates PGK1 by sponging miR-1343-3p, therefore promoting gastric cancer progression. However, the lncRNAs regulating PGK1 in breast cancer remain unknown. We found out a lncRNA LINC00926 in regulating breast cancer growth and progression. LINC00926 not only inhibits the Warburg effect but also suppresses breast tumor growth and metastasis through inhibition of PGK1-mediated Warburg effect. To our knowledge, this is the first study referring the biological function of LINC00926.

PGK1 is overexpressed in multiple types of cancers and indicates a poor prognostic marker in breast cancer, head and neck cancer, cervical cancer, liver cancer, lung cancer, colon cancers, and pancreatic cancer based on database analysis and previous findings.[4–6] Expression of PGK1 is stimulated by several known oncogenes or transcription factors, such as HIF-1α, MYC, and SIX1. Besides that, post-translational modification (PTM) for PGK1, including acetylation, phosphorylation, ubiquitination, and succinylation, is also a critical way to modulate its protein enzymatic activity. Ubiquitination, which generally promotes protein degradation, plays a critical role in both physiological and pathological processes, such as reproduction, growth and development, signal transduction, and tumorigenesis.[18–21] The conjugation of ubiquitin to cellular proteins regulates a broad range of eukaryotic cell functions. The high efficiency and exquisite selectivity of ubiquitination reactions depend on the properties of enzymes known as ubiquitin-protein ligases or E3 ligase. Dong et al.[22] performed mechanistic investigations showing that Rab11-FIP2 interacted with PGK1 and promoted its ubiquitination in NSCLC cells, leading to inactivation of the oncogenic AKT/mTOR signaling pathway. Yu et al.[11] showed that LINC00963 regulated PGK1 by blocking its ubiquitin-mediated degradation in NSCLC cells and that GBCDRlnc1 regulated PGK1 expression through inhibiting its ubiquitination.[12] However, the exact E3 ligase remains unknown. In our study, we demonstrated that LINC00926 interacts with PGK1 and promotes its ubiquitination and degradation through combining with the E3 ligase STUB1. To our knowledge, this is the first E3 ligase responsible for PGK1 degradation and may be a potential therapeutic target for breast cancer.

Another upstream factor of PGK1 in breast cancer is FOXO3A. FOXO3A is a nuclear RNA-binding protein that is involved in many cellular events. Emerging evidence indicates that FOXO3A acts as a tumor suppressor in cancer and regulate tumorigenesis

cells by combination of RNA FISH and immunofluorescence. Nuclei were stained with 4',6-Diamidine-2'-phenylindole dihydrochloride (DAPI) (blue). Scale bar, 25 μm. (C) Immunoblot analysis of MCF7 and MDA-MB-231 cells stably transfected with LINC00926 or empty vector and treated with the proteasome inhibitor MG132 (10 μM). Histograms show corresponding expression levels of LINC00926 by quantitative real-time PCR. (D) The ubiquitination of PGK1 upon LINC00926 or not were analyzed by coIP with treatment of MG132 and Myc-Ubi. (E) Ubiquitination of endogenous PGK1. Cell lysates from MCF-7 cells transfected with LINC00926 siRNA followed by immunoblotting with the indicated antibodies. Ub, ubiquitin; Scr, Scramble. The levels of ubiquitination were analyzed by western blot. Bottom, input from cell lysates. (F) Silver-stained SDS-PAGE gel of proteins immunoprecipitated by the sense and antisense of LINC00926. The differentially exhibited lanes were used for mass spectrum. (G) Immunoblotting for specific associations of STUB1 or E6AP with LINC00926 from two independent RNA pull-down assays. (H) RIP assays were performed using antibodies against PGK1 or STUB1. The mean ± SD of triplicate experiments was plotted, $^{**}p < 0.01$. (I) Effects of LINC00926 on STUB1-mediated PGK1 ubiquitination. coIP was performed in MCF-7 cells transfected with the indicated constructs and treated with 10 μM MG132. (J) MCF-7 cells treated with 10 μM MG132 and transfected with HA-Ubi, STUB1 siRNA, LINC00926, and FLAG-PGK1 were immunoprecipitated with anti-FLAG, followed by immunoblotting with the indicated antibodies. (K) coIP was performed using lysates of MCF-7 cells expressing Myc-STUB1 and FLAG-PGK1 with expression of LINC00926. (L) Immunoblot analysis of PGK1 and STUB1 in MCF-7 and MDA-MB-231 cells stably infected with EV or LINC00926 and transfected with Control siRNA or STUB1 siRNA.

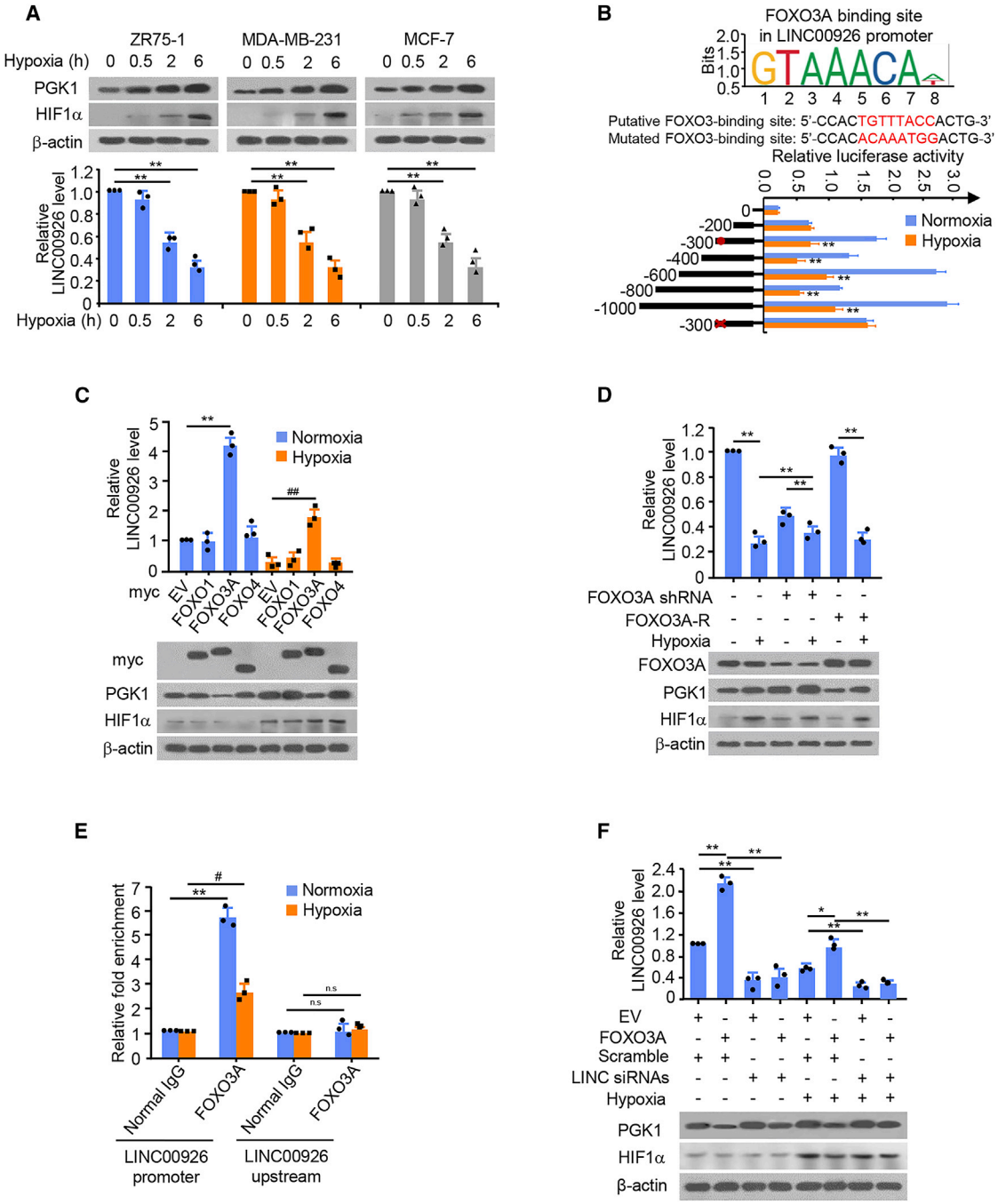

Figure 5. Hypoxia inhibits LINC00926 expression and activates PGK1 expression largely through FOXO3A transcription

(A) Quantitative real-time PCR and immunoblot analysis of ZR-751, MDA-MB-231, and MCF-7 cells exposed to normoxic (0 h) or hypoxic (0.5 h, 2 h, 6 h) conditions. Representative immunoblot shows the expression of PGK1 and HIF-1α. β-actin was used as a loading control. LINC00926 expression levels were determined by quantitative real-time PCR. (B) A conserved FOXO3A-binding element at the LINC00926 promoter was predicted by JASPAR (http://jaspar.genereg.net/). Luciferase activity of different LINC00926 promoter reporters in MCF-7 cells transfected with FOXO3A or empty vector and exposed to either normoxic or hypoxic condition. Filled circles show the position of the putative FOXO3A-binding site, and the "X" shows the mutated FOXO3A-binding site. The red letters of each binding region indicate the putative FOXO3A-binding sequences or the mutated FOXO3A-binding sequences. (C) Quantitative real-time PCR analysis of LINC00926 expression in MCF-7 cells transfected with EV, FOXO1, FOXO3A, and FOXO4 and exposed to either normoxic or hypoxic condition. Representative immunoblot shows the expression of FOXOs, PGK1, and HIF-1α. β-actin was used as an internal control. (D) Quantitative real-time PCR and immunoblot analysis of MCF-7 cells transfected with FOXO3A shRNA or FOXO3A-R under hypoxia condition or not as indicated. (E) ChIP analysis of FOXO3A occupancy on the LINC00926 promoter or upstream of the promoter in MCF-7 cells under normoxic or hypoxic condition. (F)

(legend continued on next page)

and energy metabolism in many tissues. FOXO3A plays a crucial role in apoptosis,[23] survival,[24] cell proliferation,[25] cell-cycle progression,[26] DNA damage,[27] and resistance to oxidative stress. Dysregulation of FOXO3A is highly associated with a series of malignancies.[28–31] As for breast cancer, FOXO3A is a tumor suppressor in regulating breast cancer growth and progression through multiple mechanisms. For example, Liu et al.[32] investigated that FOXO3A suppresses migration, invasion, EMT, and *in vivo* metastasis of breast cancer cells by directly inducing miR-29b-2 and miR-338 expression. He et al.[33] confirmed a suppressive role of FOXO3A in breast cancer stem cell properties and tumorigenicity. Here we explored a mechanism of FOXO3A in controlling breast cancer cell growth and progression through upregulation of LINC00926 expression; however, we couldn't deny the existence of other mechanisms. Interestingly, expression of FOXO3A was colocalized with HIF-1α expression. FOXO3A was upregulated in hypoxia, and translocation of FOXO3A from the cytoplasm to the nucleus was induced by hypoxia.[34] Some researchers demonstrated that FOXO3A was upregulated in hypoxia and translocation of FOXO3A from the cytoplasm to the nucleus was induced by hypoxia.[34,35] Others also found that hypoxia significantly downregulated the phosphorylation level of FOXO3A compared to that of normoxia, however, the total FOXO3A expression level didn't change.[36] Hence, it can be seen that the expression of FOXO3A under hypoxia condition depends on the context, which might be due to different cell lines or different ways of hypoxia (physical or chemical hypoxia manner), or different exposure time or hypoxic concentration. In our current study, we found that the expression of FOXO3A didn't change in two breast cancer cell lines, however, the recruitment of FOXO3A to LINC00926 promoter significantly decreased under hypoxia. As a consequence, the transcription of LINC00926 was inhibited and thus increased the expression of PGK1. Given the regulatory effect of LINC00926 on PGK1 and the distribution of LINC00926 (both cytoplasmic and nuclear), PGK1 (cytoplasmic), and FOXO3A (nuclear), we speculate that PGK1 is a functional downstream target of LINC00926 in the cytosol, whereas FOXO3A may function as an upstream regulator of this lincRNA in the nucleus. Our data strongly support a critical role for FOXO3A in the transcriptional activation of LINC00926.

In conclusion, our study is the first report demonstrating that LINC00926 inhibits breast cancer cell proliferation, invasion, and metastasis both *in vitro* and *in vivo* by dampening glycolysis via inhibition of PGK1 expression, a key glycolysis enzyme. LINC00926 increased by FOXO3A is negatively correlated with PGK1 expression in breast cancer patients. These findings outline the importance of the FOXO3A/LINC00926/PGK1 axis in Warburg effect and breast tumorigenesis and progression (Figure 8C). Therefore, upregulation of LINC00926 may be a promising way to treat PGK1 overexpression breast cancer patients.

MATERIALS AND METHODS

Cell lines, plasmids, lentivirus, RNA oligonucleotides, and regents

Human breast cancer cell lines MCF-7, T47D, ZR75-1, MDA-MB-453, and MDA-MB-231 cells were obtained from the American Type Culture Collection (Manassas, VA, USA). All cell lines were incubated in Dulbecco's modified Eagle's medium (DMEM) supplemented with 10% fetal bovine serum (FBS) at 37°C in a humidified atmosphere of 5% CO_2. The eukaryotic expression vectors were generated by inserting PCR-amplified fragments into pcDNA3.0 (Invitrogen). The LINC00926 promoter and its mutant luciferase reporters were made by inserting PCR-amplified promoter fragments from genomic DNA into the pGL3-Basic vector (Promega, Madison, WI, USA). Wild-type and mutated FOXO3A putative targets on LINC00926 were cloned into pGL3-Basic vector (Promega). The cDNA target sequences of small interfering RNAs (siRNAs) and/or short hairpin RNAs (shRNAs) for FOXO3A, LINC00926, and PGK1 are listed in Table S1. Lentiviral vector expressing FOXO3A, PGK1 shRNA, or LINC00926 shRNA was constructed by cloning FOXO3A, PGK1 shRNA, or LINC00926 shRNA fragments into pCDH and pSIH-H1-Puro (System Biosciences), respectively. Stable cell lines overexpressing FOXO3A plus LINC00926 shRNA were generated by infection with the lentiviruses carrying FOXO3A and LINC00926 shRNA. Stable cell lines with LINC00926 shRNA plus PGK1 shRNA were generated by infection with the lentiviruses carrying LINC00926 shRNA and PGK1 shRNA. Stable cells were selected using puromycin. Lipofectamine 2000 (Life Technologies) and Lipofectamine RNAiMAX (Life Technologies) were used for transfections of plasmids and siRNAs according to the manufacturer's instructions (Invitrogen). Anti-PGK1 was purchased from Proteintech and anti-β-actin antibodies were purchased from Santa Cruz Biotechnology.

Luciferase reporter assay

LINC00926 promoter and serial truncations were cloned into pGL3.0-basic vector/plasmid. Cells were plated at a density of 1×10^5 cells per well. Cells were co-transfected with luciferase reporters, either LINC00926 or its truncations luciferase reporter constructs containing either wild-type or mutant FOXO3A using Lipofectamine 2000. After 48 h, cells were harvested and analyzed for luciferase and β-galactosidase activities according to the manufacturer's instructions (Promega).[37] Experiments were performed in triplicate and repeated 3 times.

RNA isolation and quantitative real-time PCR

Total RNAs from cultured cells were extracted with TRIzol reagent (Invitrogen, USA) according to the manufacturer's protocol. Real-time PCR was performed using SYBR Green (BioRad) on the CFX96 system

Quantitative real-time PCR analysis of LINC00926 expression in MCF-7 cells transfected with FOXO3A or FOXO3A plus LINC00926 siRNAs and exposed to either normoxic or hypoxic condition. Representative immunoblots show the expression of PGK1 and HIF-1α. β-actin was used as a loading control. Values shown are mean ± SD of triplicate measurements that have been repeated 3 times with similar results. *$p < 0.05$, **$p < 0.01$ versus corresponding empty vector. $^{\#}p < 0.05$, $^{\#\#}p < 0.01$ versus corresponding empty vector under hypoxia.

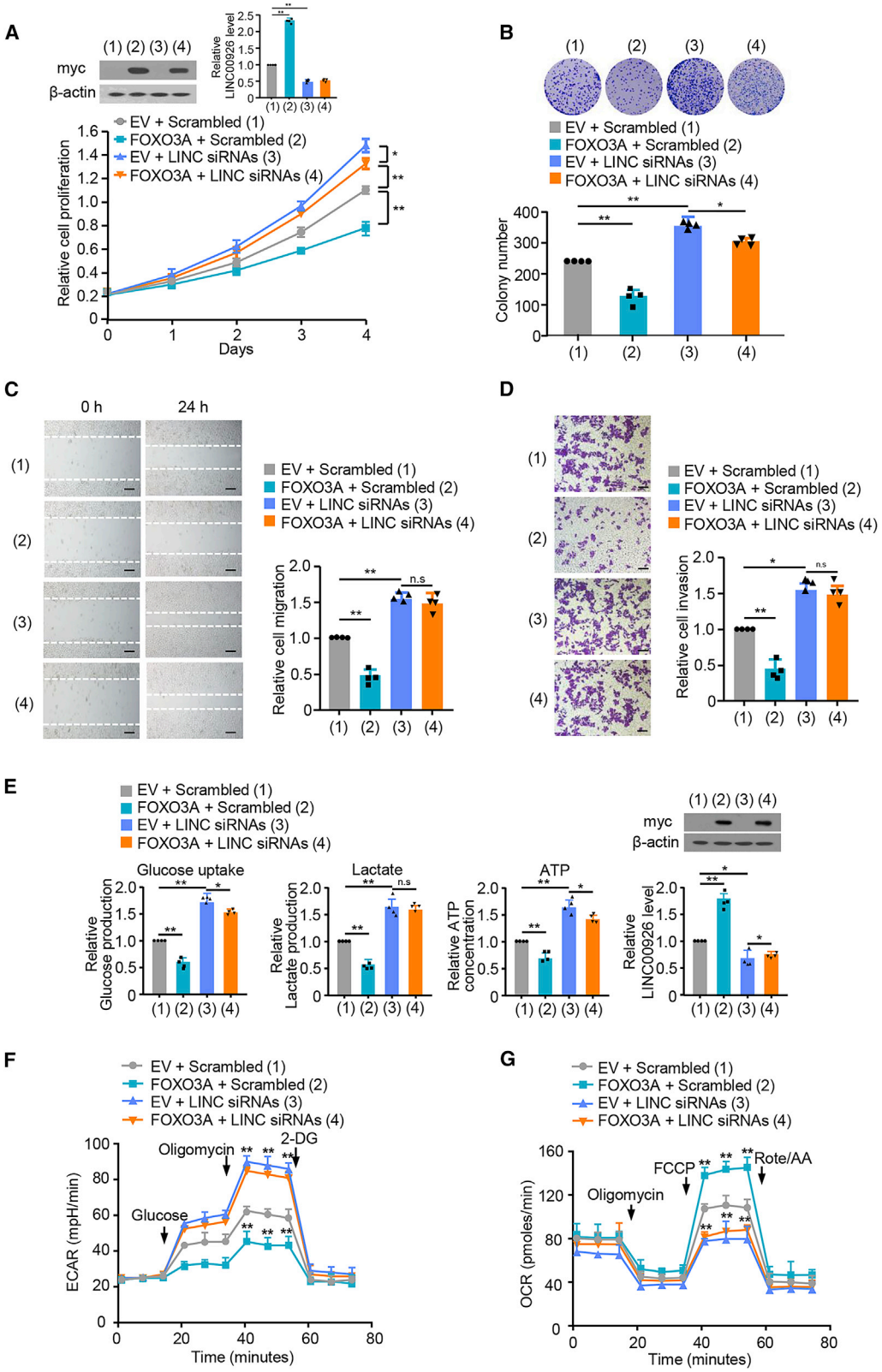

(legend on next page)

(BioRad Laboratories, Hercules, CA, USA). The relative expression of different sets of genes was normalized to β-actin. The relative fold expression of the target, normalized to the corresponding control, was calculated by the comparative *Ct* methods. Primer sequences for quantitative real-time PCR used were listed in Table S2.

Cell growth, migration, and invasion assays

For proliferation assay, cells were seeded in 96-well flat-bottomed plates with each well containing 3,000 cells and assessed by a cell counting kit-8 (CCK-8) kit according to the manufacturer's instructions (Dojindo). Colony formation was assessed with crystal violet staining after 2 weeks. The number of colonies with diameters of more than 1.5 mm was counted. Wound-healing assay was performed to detect the cell migration. Briefly, transfected cells grown to 90% confluence in 6-well plates were scratched via a 200 μL sterile pipette tip. Cells were washed with serum-free medium to remove the debris and cultured for 24 h, after which images were captured under an inverted microscope (TE2000, Nikon, China). The wound-healing rates were calculated and compared to the width at 0 h. Transwell assay was conducted to determine the cell invasion with Matrigel Invasion Chambers following the manufacturer's instructions (BD Biosciences). Briefly, cells were placed on the upper surface of the Transwell insert. After 24 h, the invasive cells were fixed with 4% paraformaldehyde and stained with 0.5% crystal violet. The number of invasive cells were counted in five randomly selected microscope visions and photographed.

Glucose uptake, lactate, and ATP assay

Glucose Uptake Colorimetric Assay kit, Lactate Assay Kit II, and ATP Colorimetric Assay kit were used to determine glucose uptake, lactate, and ATP production, respectively, according to the manufacturer's protocols (Biovision). For glucose uptake colorimetric assay, cells were seeded at a density of 1×10^6 cells per well in a 96-well plate. The cells were starved for glucose by preincubating with 100 μL Krebs-Ringer-Phosphate-HEPES (KRPH) buffer containing 2% BSA for 40 min. 10 μL of 10 mM 2-DG were added and the cells were incubated for 20 min. For lactate and ATP assays, 1×10^6 cells were homogenized in 100 μL corresponding assay buffer provided by the kits. Samples were centrifuged, and the soluble fraction was assayed. For lactate dehydrogenase activity analysis, 1×10^6 cells were lysed in 100 μL assay buffer in the kit and centrifuged at 10,000 × *g* for 15 min at 4°C.[38] 30 μL of supernatants were added to a 96-well plate.

Extracellular acidification and OCR assays

The ECAR and cellular OCR were determined using the Seahorse XFe 96 Extracellular Flux Analyzer (Seahorse Bioscience). Experiments were performed according to the manufacturer's protocols. ECAR and OCR were examined using Seahorse XF Glycolysis Stress Test Kit and Seahorse XF Cell Mito Stress Test Kit, respectively. Briefly, 1×10^4 cells per well were seeded into a Seahorse XF 96-cell culture microplate. After baseline measurements, for ECAR, glucose, the oxidative phosphorylation inhibitor oligomycin, and the glycolytic inhibitor 2-DG were sequentially injected into each well at indicated time points; and for OCR, oligomycin, the reversible inhibitor of oxidative phosphorylation FCCP (p-trifluoromethoxy carbonyl cyanide phenylhydrazone), and the mitochondrial complex I inhibitor rotenone plus the mitochondrial complex III inhibitor antimycin A (Rote/AA) were sequentially injected. Data were assessed by Seahorse XF-96 Wave software. OCR is shown in pmols/min and ECAR in mpH/min.[39]

ChIP assay

ChIP assay was performed using the Magna ChIP G Assay Kit (Millipore) according to the manufacturer's instructions. Briefly, complexes were eluted from the primary immunoprecipitation by incubation with 10 mM DTT at 37°C for 30 min and diluted 1:50 in ChIP buffer (150 mM NaCl, 1% Triton X-100, 2 mM EDTA, 20 mM Tris-HCl, pH 8.1). The immunoprecipitated DNA was amplified with a promoter pair specific for the LINC00926-promoter. The resulting values were normalized to those of the immunoglobulin G (IgG) or empty vector-infected control.[40] Primer sequences for quantitative real-time PCR used were listed in Table S3.

Cytosolic and nuclear fractionation

MCF-7 and MDA-MB-231 cells were washed with PBS twice and incubated with lysis buffer (25 mM Tris-HCl, pH 7.4, 1 mM $MgCl_2$, 5 mM KCl, and 1% NP-40) on ice for 10 min. The supernatant of the cell lysates was collected as the cytoplasmic fraction at 2,000 × rpm for 10 min. Then the pellets were resuspended in nucleus resuspension buffer (20 mM HEPES, pH 7.9, 400 mM NaCl, 1 mM EDTA, 1 mM EGTA, 1 mM DTT, 1 mM PMSF) for 30 min. After centrifugation at 12,000 × rpm for 10 min, the supernatant was collected as the nuclear fraction. Cytoplasmic and nuclear fractions were divided for RNA extraction. 18S and U6 were used as quantitative real-time PCR markers of cytoplasmic and nuclear RNAs, respectively.

RNA pull-down and mass spectrometry analysis

Biotin-labeled LINC00926 was synthesized using the Biotin RNA Labeling Mix by T7 RNA polymerase and then incubated with the cell lysates for 4 h and was pulled down with streptavidin magnetic beads (MCE) after incubation overnight. The samples were separated using electrophoresis, and the specific bands were identified using mass spectrometry and retrieved in human proteomic library.[41]

Figure 6. FOXO3A suppresses proliferation, migration, and invasion and dampens glycolysis via LINC00926 expression in breast cancer cells

(A) MCF-7 cells were transfected with myc-FOXO3A or myc-FOXO3A plus LINC siRNAs. The proliferation of the cells was detected by CCK-8 assay. The representative immunoblot shows myc-FOXO3A expression. Histograms show LINC00926 expression determined by quantitative real-time PCR. (B) Colony-formation assay of MCF-7 cells transfected as in (A). Representative images show colonies in plates (upper panels). Histograms show colony number. (C and D) Wound healing (C) and invasion (D) assays of MCF-7 cells transfected as in (A). Right histograms show relative cell migration and invasion. (E) Glucose uptake and the production of lactate and ATP were determined. Representative immunoblot reveals the expression of myc-FOXO3A. Quantitative real-time PCR analysis indicates LINC00926 expression. (F and G) MCF-7 cells were transfected as in (A), and ECAR (F) and OCR (G) were then determined.

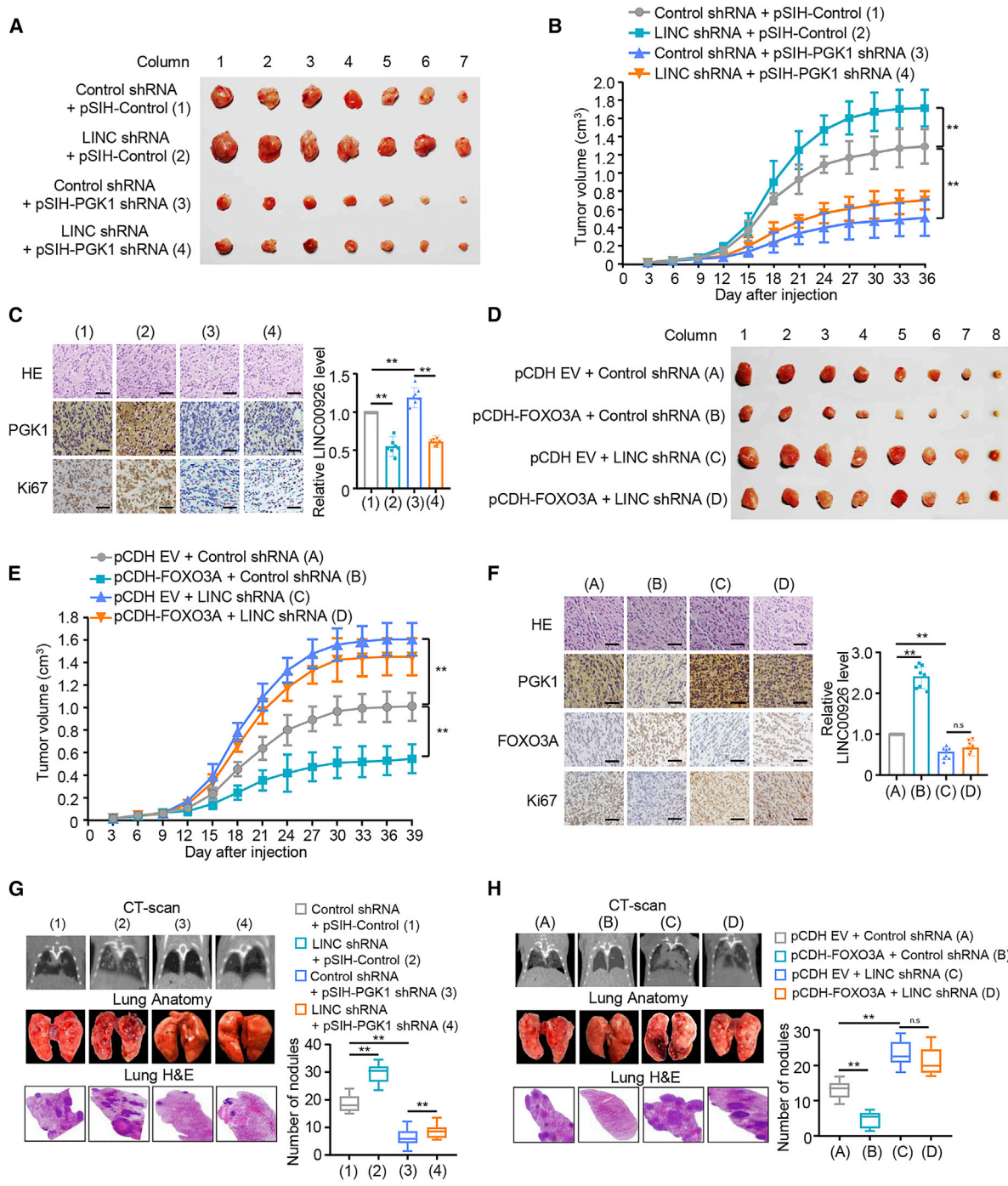

Figure 7. FOXO3A/LINC00926/PGK1 axis regulates breast cancer tumor growth and lung metastasis

(A and B) MDA-MB-231 cells stably infected with lentivirus carrying the indicated constructs were injected into subcutaneous of nude mice (n = 7 per group). At the indicated times, tumors were measured and the growth curve was plotted (B). (C) Representative IHC staining for PGK1, Ki67, and H&E images of excised tumors from (A) are shown. Scale bar, 100 μm. Histograms show LINC00926 expression determined by quantitative real-time PCR. (D–F) MDA-MB-231 cells stably infected with lentivirus carrying the indicated constructs were injected into subcutaneous of nude mice (n = 8 per group) and analyzed as in (A)–(C). (G and H) Breast cancer cell metastatic model was established in nude mice (n = 6) by tail vein injection of MDA-MB-231 cells stably expressing of indicated constructs. Lung CT scan of groups were performed and representative metastatic foci of lungs were subjected to anatomical and histological analyses. The number of tumor nodules was examined under an anatomical microscope. Symbols represent individual mice; horizontal bars indicate the mean ± SD. Scale bar, 100 μm. *p < 0.05 versus corresponding control.

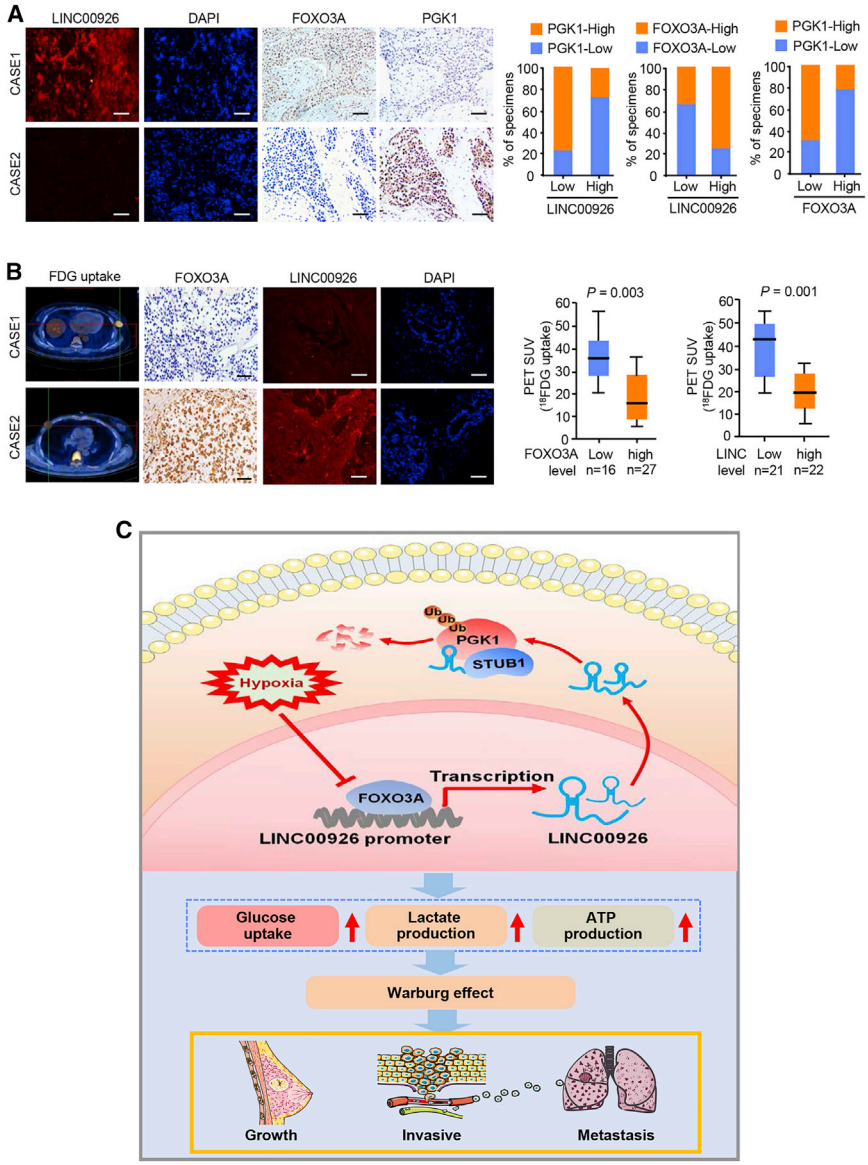

Figure 8. Correlation between LINC00926 and PGK1 expression and association of LINC00926 with glucose uptake in human breast cancer patients

(A) Representative IHC staining for FOXO3A and PGK1 and FISH staining for LINC00926 in breast cancer patients. Scale bar, 50 μm. Right panel showing the percentage of specimens with low or high PGK1 and FOXO3A expressions in the low or high LINC00926 expression groups, or low or high PGK1 in the low or high FOXO3A expression groups. CASE 1 and CASE 2 refer to two representative samples categorized by high and low LINC00926 expression. (B) The correlation of glucose uptake in breast cancer patients with FOXO3A and LINC00926 was determined using the Mann Whitney *U* test. CASE 1 and CASE 2 refer to two representative samples categorized by high and low FDG uptake. (C) Graphical abstract underlying the role of the FOXO3A/LINC00926/PGK1 in regulating breast cancer growth and lung metastasis.

Analysis of tumor growth and metastasis *in vivo*

Animal studies were approved by the Institutional Animal Care Committee of Beijing Institute of Biotechnology. For tumor growth study, a total of 1×10^7 MDA-MB-231 cells carrying different constructs were subcutaneously inoculated into the second mammary fat pad on the right side of nude mice (seven in each group). Tumor size was measured at the indicated times using calipers. Tumor volume was estimated according to the following formula: volume = (longest diameter × shortest diameter2)/2.[42] The mice were sacrificed at the indicated time. Excised tumors were frozen in liquid nitrogen for further study.

For lung metastasis study, 1×10^6 MDA-MB-231 cells carrying indicated constructs were injected into the lateral tail vein of BALB/c female mice. To investigate the lung metastasis, we maintained all mice for about 40 days until analysis by computed tomography (CT) scan. After sacrifice, all the lungs were excised for metastatic foci analysis.

Tissue samples and IHC

109 human breast cancer samples were obtained from Harbin Medical University Cancer Hospital and Affiliated Cancer Hospital & Institute of Guangzhou Medical University, with the informed consent of patients and with approval for experiments from the hospital. None of the patients had received any chemotherapy prior to surgery. All patients were female with 30–75 years of age (mean age: 51.9 years). Tumor tissue was obtained from patients undergoing surgery and immediately stored at −80°C. Tissue samples were used for IHC analysis. All IHC staining was assessed by two independent pathologists with no prior knowledge of patient characteristics. The widely accepted H-score system was used in considering the staining intensity and extent of staining area. Briefly, H-score was generated by adding the percentage of strongly stained cells (times 3), the percentage of moderately stained cells (times 2), and the percentage of weakly stained cells (times 1).

Formalin fixed and paraffin embedded tissue sections were subjected to IHC as previously described.[43] (Tissue sections were deparaffinized, rehydrated, and treated with 3% H_2O_2 for 15 min to inhibit endogenous peroxidase activity. Following heat-induced epitope retrieval in 10 mM citrate buffer [pH 6.0] in a microwave for 30 min, the slides were incubated at 4°C overnight with a prediluted primary antibody [Anti-Ki67 Servicebio (GB13030-2, China), anti-PGK1 (1:1,000, Proteintech,

17811-1-AP), anti-FOXO3A (1:5,000, Proteintech, Cat No. 66428-1-Ig)]. After incubation with a secondary antibody, the signal was developed with 3, 3′-diaminobenzidine tetrachloride.)

FISH

MCF-7 and MDA-MB-231 were rinsed briefly in 1 × PBS and then fixed in 4% paraformaldehyde for 10 min at room temperature. Cells were permeabilized in 1 × PBS containing 0.5% Triton X-100 for 5 min at 4°C, then washed in 1 × PBS for 5 min. 200 μL of pre-hybridization buffer was added at 37°C for 30 min. Hybridization was carried out with a FISH probe in a moist chamber at 37°C in the dark overnight using Ribo FISH Kit (C10910, RiboBio). The slides were washed three times with wash buffer I (4 × SSC with 0.1% Tween 20), once each with wash buffer II (2 × SSC), wash buffer III (1 × SSC) at 42°C in the dark for 5 min, and once with 1 × PBS at room temperature. Then the cells were stained with DAPI in the dark for 10 min. LINC00926 FISH probes were designed and synthesized by RiboBio Company. Human U6 FISH probes and 18S FISH probes were used as the nuclear and cytoplasmic internal controls, respectively. For breast cancer tissues, lncRNA FISH on paraffin tissue sections with probes specific for human LINC00926 was performed according to the manufacturer's instructions (RiboBio, Guangzhou, China). All images were observed by fluorescence or confocal microscope (Nikon).

Statistical analysis

Statistical analyses were performed using SPSS v.23.0 (SPSS) or Prism GraphPad 8.0. All the experiments *in vitro* were performed in triplicate and repeated 3 or 4 times. Statistical significance in cell proliferation, migration, and invasion assays, as well as luciferase reporter assays, was determined by two-tailed Student's t test. Spearman correlation analysis was performed to assess the relationship between different factors using GraphPad Prism 8.0. Differences were considered to be statistically significant at $p < 0.05$.

Ethics approval and consent to participate

This study was reviewed and approved by the Ethics Committee of Department of Medical Oncology, Harbin Medical University Cancer Hospital & Institute of Guangzhou Medical University, and all the participants signed an informed consent form.

SUPPLEMENTAL INFORMATION

Supplemental information can be found online at https://doi.org/10.1016/j.ymthe.2021.04.036.

ACKNOWLEDGMENTS

This work was supported by grants from the National Natural Science Foundation of China (81822037, 81972446, 81672602, 81872090, and 81730074, 81903088, 81911530169, and 81602534), Beijing Science Foundation for Distinguished Young Scholars (JQ19028), Beijing Science Foundation (7192196), the Logistics Scientific Research project (BWS16J010), and the Key Basic Research project of Basic Strengthening Program (2020-JCJQ-ZD-253-04). Harbin Medical University Cancer Hospital and Beijing Institute of Biotechnology made equal contributions to this work.

AUTHOR CONTRIBUTIONS

X.X. conceived the project, designed the experiments, and analyzed the data; Q.Z. supervised the project; Z.C. designed and performed the experiments and analyzed the data; N.H., X.Z., H.L., and R.C. performed the experiments and analyzed the data; N.H. performed CT scan analysis; N.H., L.M., X.K., and C.X. made expression vectors and performed animal experiments; H.Y., Q.L., and Q.Z. collected and analyzed the clinical samples; X.X. and Z.C. wrote the manuscript.

DECLARATION OF INTERESTS

The authors declare no competing interests.

REFERENCES

1. Hanahan, D., and Weinberg, R.A. (2011). Hallmarks of cancer: the next generation. Cell *144*, 646–674.
2. Hu, H., Zhu, W., Qin, J., Chen, M., Gong, L., Li, L., Liu, X., Tao, Y., Yin, H., Zhou, H., et al. (2017). Acetylation of PGK1 promotes liver cancer cell proliferation and tumorigenesis. Hepatology *65*, 515–528.
3. Daly, E.B., Wind, T., Jiang, X.M., Sun, L., and Hogg, P.J. (2004). Secretion of phosphoglycerate kinase from tumour cells is controlled by oxygen-sensing hydroxylases. Biochim. Biophys. Acta *1691*, 17–22.
4. Tang, S.J., Ho, M.Y., Cho, H.C., Lin, Y.C., Sun, G.H., Chi, K.H., Wang, Y.S., Jhou, R.S., Yang, W., and Sun, K.H. (2008). Phosphoglycerate kinase 1-overexpressing lung cancer cells reduce cyclooxygenase 2 expression and promote anti-tumor immunity in vivo. Int. J. Cancer *123*, 2840–2848.
5. Ahmad, S.S., Glatzle, J., Bajaeifer, K., Bühler, S., Lehmann, T., Königsrainer, I., Vollmer, J.P., Sipos, B., Ahmad, S.S., Northoff, H., et al. (2013). Phosphoglycerate kinase 1 as a promoter of metastasis in colon cancer. Int. J. Oncol. *43*, 586–590.
6. Chen, G., Gharib, T.G., Wang, H., Huang, C.C., Kuick, R., Thomas, D.G., Shedden, K.A., Misek, D.E., Taylor, J.M., Giordano, T.J., et al. (2003). Protein profiles associated with survival in lung adenocarcinoma. Proc. Natl. Acad. Sci. USA *100*, 13537–13542.
7. Kress, S., Stein, A., Maurer, P., Weber, B., Reichert, J., Buchmann, A., Huppert, P., and Schwarz, M. (1998). Expression of hypoxia-inducible genes in tumor cells. J. Cancer Res. Clin. Oncol. *124*, 315–320.
8. Xu, D., Aka, J.A., Wang, R., and Lin, S.X. (2017). 17beta-hydroxysteroid dehydrogenase type 5 is negatively correlated to apoptosis inhibitor GRP78 and tumor-secreted protein PGK1, and modulates breast cancer cell viability and proliferation. J. Steroid Biochem. Mol. Biol. *171*, 270–280.
9. Geisler, S., and Coller, J. (2013). RNA in unexpected places: long non-coding RNA functions in diverse cellular contexts. Nat. Rev. Mol. Cell Biol. *14*, 699–712.
10. Sun, W., Li, A.Q., Zhou, P., Jiang, Y.Z., Jin, X., Liu, Y.R., Guo, Y.J., Yang, W.T., Shao, Z.M., and Xu, X.E. (2018). DSCAM-AS1 regulates the G_1/S cell cycle transition and is an independent prognostic factor of poor survival in luminal breast cancer patients treated with endocrine therapy. Cancer Med. *7*, 6137–6146.
11. Yu, T., Zhao, Y., Hu, Z., Li, J., Chu, D., Zhang, J., Li, Z., Chen, B., Zhang, X., Pan, H., et al. (2017). MetaLnc9 Facilitates Lung Cancer Metastasis via a PGK1-Activated AKT/mTOR Pathway. Cancer Res. *77*, 5782–5794.
12. Cai, Q., Wang, S., Jin, L., Weng, M., Zhou, D., Wang, J., Tang, Z., and Quan, Z. (2019). Long non-coding RNA GBCDRlnc1 induces chemoresistance of gallbladder cancer cells by activating autophagy. Mol. Cancer *18*, 82.
13. Cao, C., Zhong, Q., Lu, L., Huang, B., Li, J., Meng, L., and Wei, H. (2020). Long non-coding RNA MSC-AS1 promotes hepatocellular carcinoma oncogenesis via inducing the expression of phosphoglycerate kinase 1. Cancer Med. *9*, 5174–5184.
14. Wang, L., Bo, X., Yi, X., Xiao, X., Zheng, Q., Ma, L., and Li, B. (2020). Exosome-transferred LINC01559 promotes the progression of gastric cancer via PI3K/AKT signaling pathway. Cell Death Dis. *11*, 723.
15. Payen, V.L., Porporato, P.E., Baselet, B., and Sonveaux, P. (2016). Metabolic changes associated with tumor metastasis, part 1: tumor pH, glycolysis and the pentose phosphate pathway. Cell. Mol. Life Sci. *73*, 1333–1348.

16. Zhang, Y., Cai, H., Liao, Y., Zhu, Y., Wang, F., and Hou, J. (2020). Activation of PGK1 under hypoxic conditions promotes glycolysis and increases stem cell-like properties and the epithelial-mesenchymal transition in oral squamous cell carcinoma cells via the AKT signalling pathway. Int. J. Oncol. *57*, 743–755.

17. Min, H.Y., Pei, H., Hyun, S.Y., Boo, H.J., Jang, H.J., Cho, J., Kim, J.H., Son, J., and Lee, H.Y. (2020). Potent Anticancer Effect of the Natural Steroidal Saponin Gracillin Is Produced by Inhibiting Glycolysis and Oxidative Phosphorylation-Mediated Bioenergetics. Cancers (Basel) *12*, 913.

18. Cheng, X., Hao, Y., Shu, W., Zhao, M., Zhao, C., Wu, Y., Peng, X., Yao, P., Xiao, D., Qing, G., et al. (2017). Cell cycle-dependent degradation of the methyltransferase SETD3 attenuates cell proliferation and liver tumorigenesis. J. Biol. Chem. *292*, 9022–9033.

19. Bushweller, J.H. (2019). Targeting transcription factors in cancer - from undruggable to reality. Nat. Rev. Cancer *19*, 611–624.

20. Craney, A., and Rape, M. (2013). Dynamic regulation of ubiquitin-dependent cell cycle control. Curr. Opin. Cell Biol. *25*, 704–710.

21. Zhang, X., Zhang, H., Xu, C., Li, X., Li, M., Wu, X., Pu, W., Zhou, B., Wang, H., Li, D., et al. (2019). Ubiquitination of RIPK1 suppresses programmed cell death by regulating RIPK1 kinase activation during embryogenesis. Nat. Commun. *10*, 4158.

22. Dong, W., Li, H., and Wu, X. (2019). Rab11-FIP2 suppressed tumor growth via regulation of PGK1 ubiquitination in non-small cell lung cancer. Biochem. Biophys. Res. Commun. *508*, 60–65.

23. Chen, Y.F., Pandey, S., Day, C.H., Chen, Y.F., Jiang, A.Z., Ho, T.J., Chen, R.J., Padma, V.V., Kuo, W.W., and Huang, C.Y. (2018). Synergistic effect of HIF-1α and FoxO3a trigger cardiomyocyte apoptosis under hyperglycemic ischemia condition. J. Cell. Physiol. *233*, 3660–3671.

24. Joseph, J., Ametepe, E.S., Haribabu, N., Agbayani, G., Krishnan, L., Blais, A., and Sad, S. (2016). Inhibition of ROS and upregulation of inflammatory cytokines by FoxO3a promotes survival against Salmonella typhimurium. Nat. Commun. *7*, 12748.

25. McClelland Descalzo, D.L., Satoorian, T.S., Walker, L.M., Sparks, N.R., Pulyanina, P.Y., and Zur Nieden, N.I. (2016). Glucose-Induced Oxidative Stress Reduces Proliferation in Embryonic Stem Cells via FOXO3A/β-Catenin-Dependent Transcription of p21(cip1). Stem Cell Reports *7*, 55–68.

26. McGowan, S.E., and McCoy, D.M. (2013). Platelet-derived growth factor-A regulates lung fibroblast S-phase entry through p27(kip1) and FoxO3a. Respir. Res. *14*, 68.

27. Fluteau, A., Ince, P.G., Minett, T., Matthews, F.E., Brayne, C., Garwood, C.J., Ratcliffe, L.E., Morgan, S., Heath, P.R., Shaw, P.J., et al.; MRC Cognitive Function Ageing Neuropathology Study Group (2015). The nuclear retention of transcription factor FOXO3a correlates with a DNA damage response and increased glutamine synthetase expression by astrocytes suggesting a neuroprotective role in the ageing brain. Neurosci. Lett. *609*, 11–17.

28. Shoeb, M., Ramana, K.V., and Srivastava, S.K. (2013). Aldose reductase inhibition enhances TRAIL-induced human colon cancer cell apoptosis through AKT/FOXO3a-dependent upregulation of death receptors. Free Radic. Biol. Med. *63*, 280–290.

29. Shukla, S., Bhaskaran, N., Maclennan, G.T., and Gupta, S. (2013). Deregulation of FoxO3a accelerates prostate cancer progression in TRAMP mice. Prostate *73*, 1507–1517.

30. Thépot, S., Lainey, E., Cluzeau, T., Sébert, M., Leroy, C., Adès, L., Tailler, M., Galluzzi, L., Baran-Marszak, F., Roudot, H., et al. (2011). Hypomethylating agents reactivate FOXO3A in acute myeloid leukemia. Cell Cycle *10*, 2323–2330.

31. Yamamura, Y., Lee, W.L., Inoue, K., Ida, H., and Ito, Y. (2006). RUNX3 cooperates with FoxO3a to induce apoptosis in gastric cancer cells. J. Biol. Chem. *281*, 5267–5276.

32. Song, Y., Zeng, S., Zheng, G., Chen, D., Li, P., Yang, M., Luo, K., Yin, J., Gu, Y., Zhang, Z., et al. (2021). FOXO3a-driven miRNA signatures suppresses VEGF-A/NRP1 signaling and breast cancer metastasis. Oncogene *40*, 777–790.

33. Liu, H., Song, Y., Qiu, H., Liu, Y., Luo, K., Yi, Y., Jiang, G., Lu, M., Zhang, Z., Yin, J., et al. (2020). Downregulation of FOXO3a by DNMT1 promotes breast cancer stem cell properties and tumorigenesis. Cell Death Differ. *27*, 966–983.

34. Brucker, D.P., Maurer, G.D., Harter, P.N., Rieger, J., and Steinbach, J.P. (2016). FOXO3a orchestrates glioma cell responses to starvation conditions and promotes hypoxia-induced cell death. Int. J. Oncol. *49*, 2399–2410.

35. Jensen, K.S., Binderup, T., Jensen, K.T., Therkelsen, I., Borup, R., Nilsson, E., Multhaupt, H., Bouchard, C., Quistorff, B., Kjaer, A., et al. (2011). FoxO3A promotes metabolic adaptation to hypoxia by antagonizing Myc function. EMBO J. *30*, 4554–4570.

36. Liang, C., Dong, Z., Cai, X., Shen, J., Xu, Y., Zhang, M., Li, H., Yu, W., and Chen, W. (2020). Hypoxia induces sorafenib resistance mediated by autophagy via activating FOXO3a in hepatocellular carcinoma. Cell Death Dis. *11*, 1017.

37. Xiu, B., Chi, Y., Liu, L., Chi, W., Zhang, Q., Chen, J., Guo, R., Si, J., Li, L., Xue, J., et al. (2019). LINC02273 drives breast cancer metastasis by epigenetically increasing AGR2 transcription. Mol. Cancer *18*, 187.

38. Shang, R., Wang, M., Dai, B., Du, J., Wang, J., Liu, Z., Qu, S., Yang, X., Liu, J., Xia, C., et al. (2020). Long noncoding RNA SLC2A1-AS1 regulates aerobic glycolysis and progression in hepatocellular carcinoma via inhibiting the STAT3/FOXM1/GLUT1 pathway. Mol. Oncol. *14*, 1381–1396.

39. Zhangyuan, G., Wang, F., Zhang, H., Jiang, R., Tao, X., Yu, D., Jin, K., Yu, W., Liu, Y., Yin, Y., et al. (2020). VersicanV1 promotes proliferation and metastasis of hepatocellular carcinoma through the activation of EGFR-PI3K-AKT pathway. Oncogene *39*, 1213–1230.

40. Lu, G., Li, Y., Ma, Y., Lu, J., Chen, Y., Jiang, Q., Qin, Q., Zhao, L., Huang, Q., Luo, Z., et al. (2018). Long noncoding RNA LINC00511 contributes to breast cancer tumourigenesis and stemness by inducing the miR-185-3p/E2F1/Nanog axis. J. Exp. Clin. Cancer Res. *37*, 289.

41. Wen, X., Liu, X., Mao, Y.P., Yang, X.J., Wang, Y.Q., Zhang, P.P., Lei, Y., Hong, X.H., He, Q.M., Ma, J., et al. (2018). Long non-coding RNA DANCR stabilizes HIF-1α and promotes metastasis by interacting with NF90/NF45 complex in nasopharyngeal carcinoma. Theranostics *8*, 5676–5689.

42. Kim, N.H., Cha, Y.H., Lee, J., Lee, S.H., Yang, J.H., Yun, J.S., Cho, E.S., Zhang, X., Nam, M., Kim, N., et al. (2017). Snail reprograms glucose metabolism by repressing phosphofructokinase PFKP allowing cancer cell survival under metabolic stress. Nat. Commun. *8*, 14374.

43. Wang, J., Cheng, P., Pavlyukov, M.S., Yu, H., Zhang, Z., Kim, S.H., Minata, M., Mohyeldin, A., Xie, W., Chen, D., et al. (2017). Targeting NEK2 attenuates glioblastoma growth and radioresistance by destabilizing histone methyltransferase EZH2. J. Clin. Invest. *127*, 3075–3089.